Postnatal NMDA receptor ablation in corticolimbic interneurons confers schizophrenia-like phenotypes

Juan E. Belforte, Veronika Zsiros, Elyse R. Sklar, Zhihong Jiang, Gu Yu, Yuqing Li, Elizabeth M. Quinlan & Kazu Nakazawa

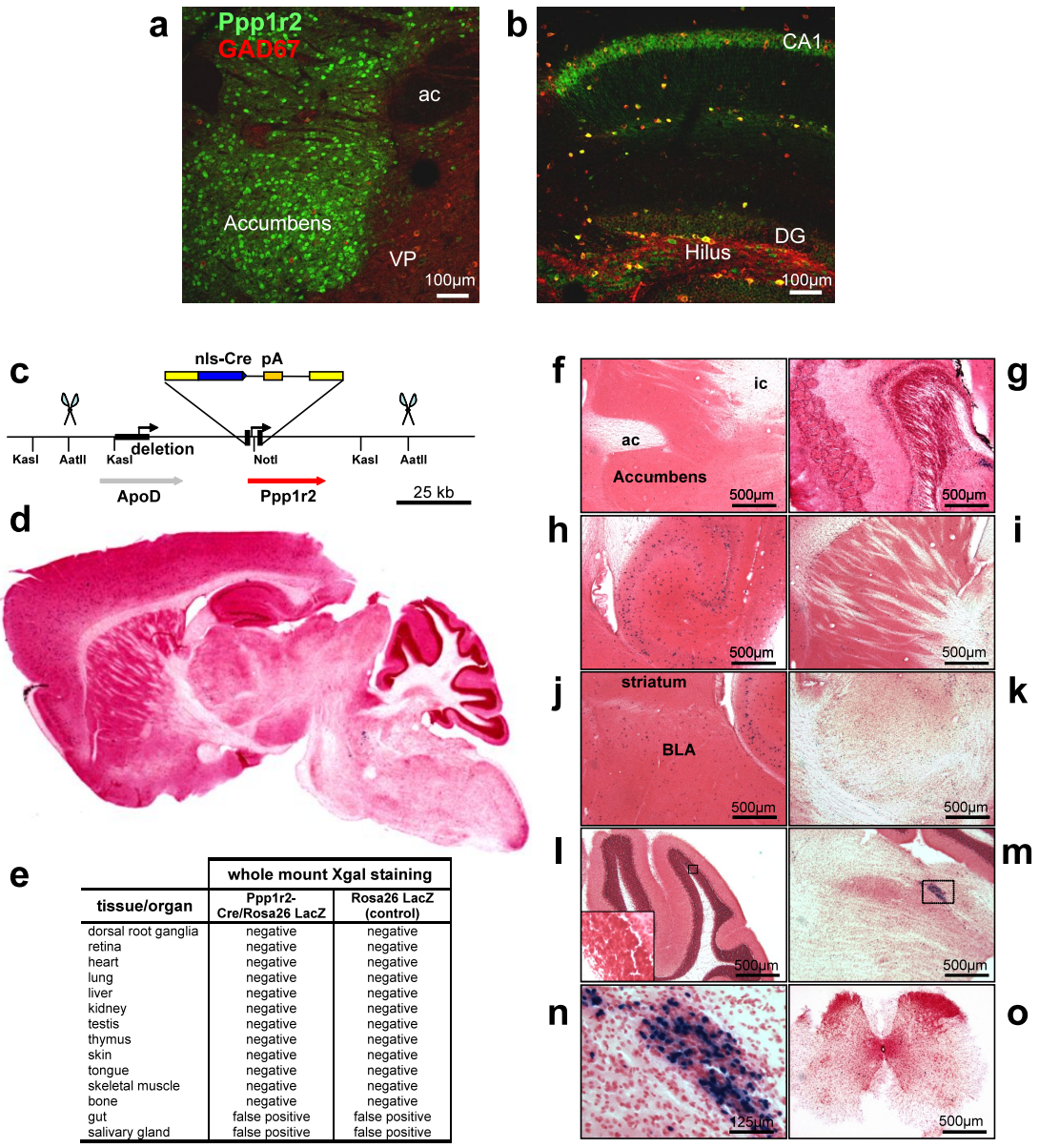

tissue/organ	whole mount Xgal staining	
	Ppp1r2-Cre/Rosa26 LacZ	Rosa26 LacZ (control)
dorsal root ganglia	negative	negative
retina	negative	negative
heart	negative	negative
lung	negative	negative
liver	negative	negative
kidney	negative	negative
testis	negative	negative
thymus	negative	negative
skin	negative	negative
tongue	negative	negative
skeletal muscle	negative	negative
bone	negative	negative
gut	false positive	false positive
salivary gland	false positive	false positive

Supplementary Fig. 1 Generation and characterization of *Ppp1r2-Cre* mice. (**a-b**) Endogenous Ppp1r2 immunoreactivity in 4-week-old wild type C57BL/6N mouse. Confocal photomicrographs from parasagittal sections double-immunostained with anti-Ppp1r2 (Alexa 488: green) and anti-GAD67 (Cy3: red). (**a**) Nucleus accumbens, (**b**) hippocampus, ac, anterior commissure; VP, ventral pallidum; pia, dorsal pia mater; DG, dentate gyrus. Note that Ppp1r2 protein is highly expressed in medium spiny neurons in the striatum, where GAD65 is more abundant than GAD67. (**c**) Schematic representation of BAC DNA construct used for generating the transgenic *Ppp1r2-Cre* (Cre #4127) line. A cDNA fragment carrying nuclear localization signal(nls)-fused Cre recombinase followed by human growth hormone polyA signal was inserted just upstream of the initial Met of the *Ppp1r2*

Nature Neuroscience: doi:10.1038/nn.2447

coding region (red arrow) following BAC using homologous recombination in *E. coli*. A region in the *ApoD* gene (thick black bar) was deleted to avoid potential overexpression of the *ApoD* gene product. The DNA fragment excised for oocyte injection is flanked by scissors. nls: nuclear localization signal. (**d**) Spatial distribution of Cre recombinase activity in the *Ppp1r2-Cre* mice. A parasagittal section from *Ppp1r2-Cre;Rosa26LacZ*[1] double-transgenic mouse (8-week-old) stained with X-Gal (blue) for β-galactosidase activity and counterstained with Safranin O (red). Note the scattered distribution of Cre-targeted neurons across cortex and hippocampus. (**e**) Whole mount X-Gal staining from the same animal in (**d**), showing no detectable Cre-recombination outside the brain. (**f** – **o**) High magnification microphotographs of parasagittal sections of the same animal, (**f**) Nucleus accumbens; (**g**) olfactory bulb; (**h**) ventral hippocampus; (**i**) striatum; (**j**) basolateral amygdala (BLA); (**k**) thalamus; (**l**) cerebellum; (**m** and **n**), nucleus tractus solitaris (NTS); (**o**) spinal cord. Note that the *lacZ* expression was sporadically detected in some cell-types at 8-week-old (~30% of NTS; ~3% of dentate granule cells; ~5% of GAD67-positive interneurons in striatum and amygdala). Glial expression of Cre recombinase was observed with extremely low frequency (approximately 40 glial cells per whole brain), as revealed by morphological and immunocytochemical analyses (data not shown)**.**

Nature Neuroscience: doi:10.1038/nn.2447

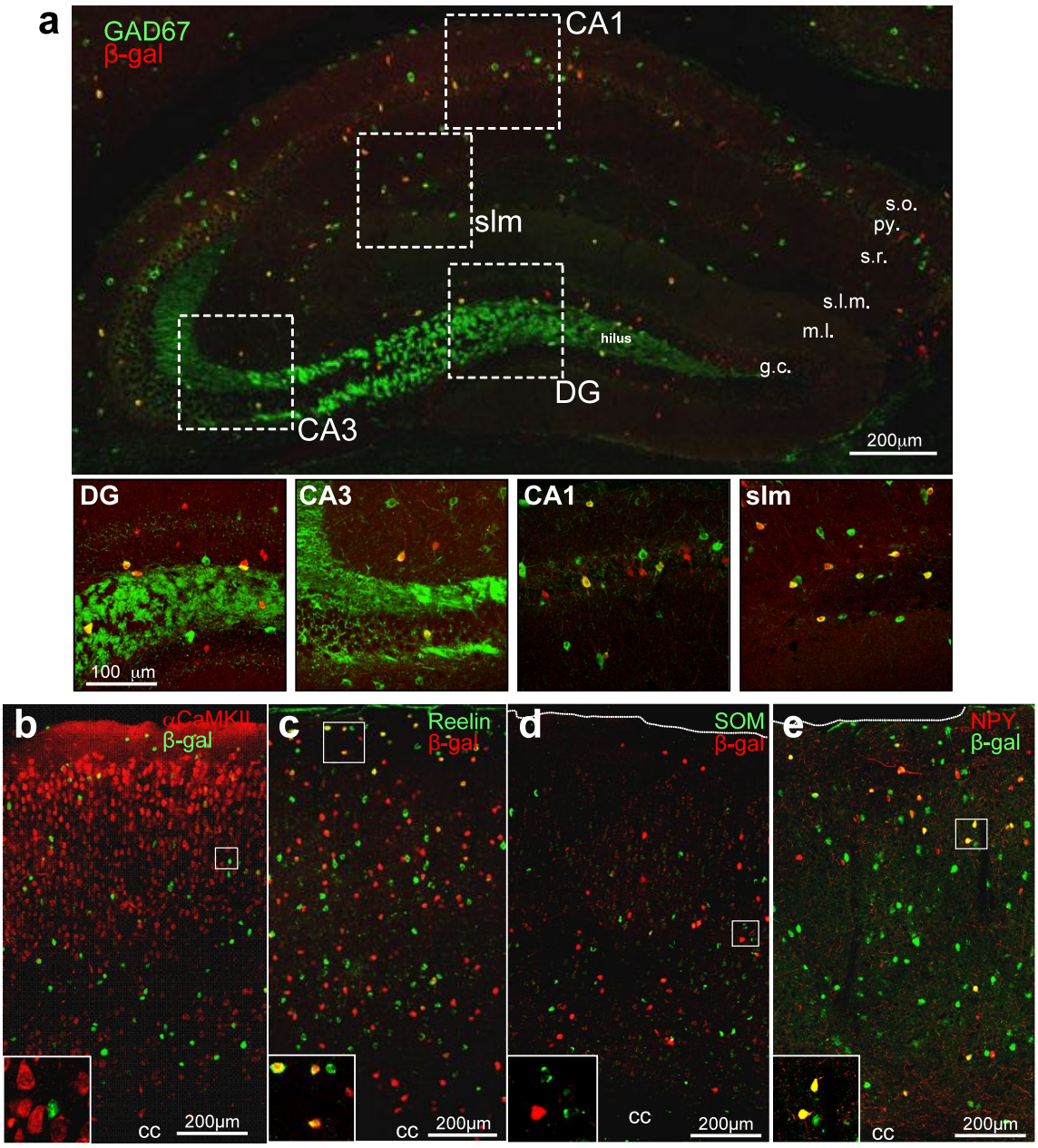

Supplementary Fig. 2 Neuron type-specific recombination pattern in *Ppp1r2-Cre/Rosa26LacZ* mice. (**a**) Confocal images of double immunofluorescence in hippocampus from 8-week-old male *Ppp1r2-Cre/Rosa26LacZ* mice. Targeted neurons were identified by anti-β-galactosidase (β-gal). GABAergic neurons were detected with anti-GAD67. so: stratum oriens, py: pyramidal layer, sr: stratum radiatum, slm: stratum lacunosum moleculare, ml: molecular layer, gc: granule cells. (**b** to **e**) Coronal sections from somatosensory cortex immunostained for β-galactosidase in different colors (red: Cy3, green: Alexa 488) and αCaMKII (**b**, excitatory cell marker[2]) and interneuron markers [Reelin in (**c**), somatostatin (SOM) in (**d**), and neuropeptide Y (NPY) in (**e**)]. High magnifications of boxed areas are shown in the lower right corner. As only a small fraction of Cre-targeted neurons (~1-3%) was SOM-positive and no CR-positive in the Cre-targeted neurons, Reelin-positive cells may largely represent late-spiking neurons derived from caudal ganglionic eminence. Note that Reelin-positive neurons do not overlap with PV-positive neurons in mice (G. Miyoshi and G. Fishell, personal communication). cc: corpus callosum.

Nature Neuroscience: doi:10.1038/nn.2447

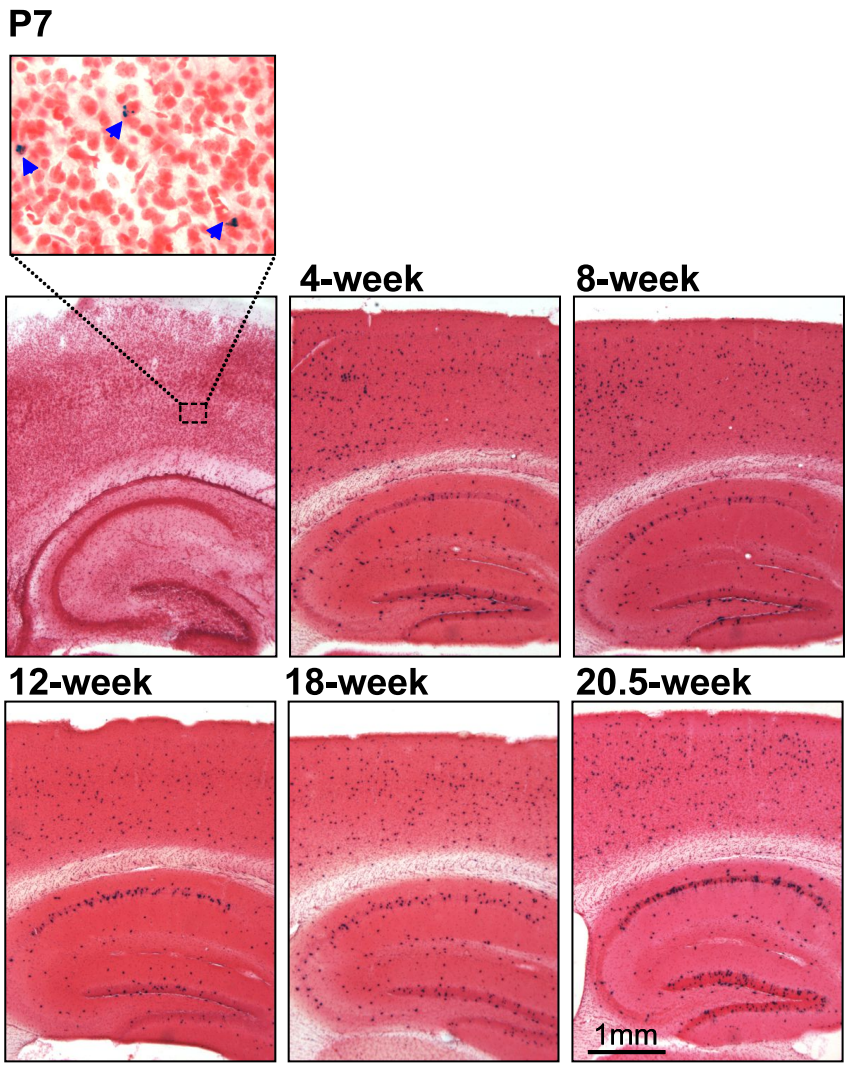

Supplementary Fig. 3 Temporal pattern of Cre-recombination in *Ppp1r2-Cre/Rosa26LacZ* mice. Developmental profile of Cre-mediated recombination by X-Gal staining (blue) from parasagittal sections through hippocampus and cortex counterstained with Safranin O (red). Cre-recombination in GABAergic interneurons started in cortex and hippocampus at postnatal day 7 (blue arrows) and remained stable from 4 to 18 weeks of age. A sporadic expression of Cre-recombinase was also detected in CA1 pyramidal cells at extremely low frequency (5 to 7 cells per 50-μm thickness section) from 8 to 12 weeks of age. The sporadic expression in CA1 pyramidal cells began to expand around 20 weeks of age.

Nature Neuroscience: doi:10.1038/nn.2447

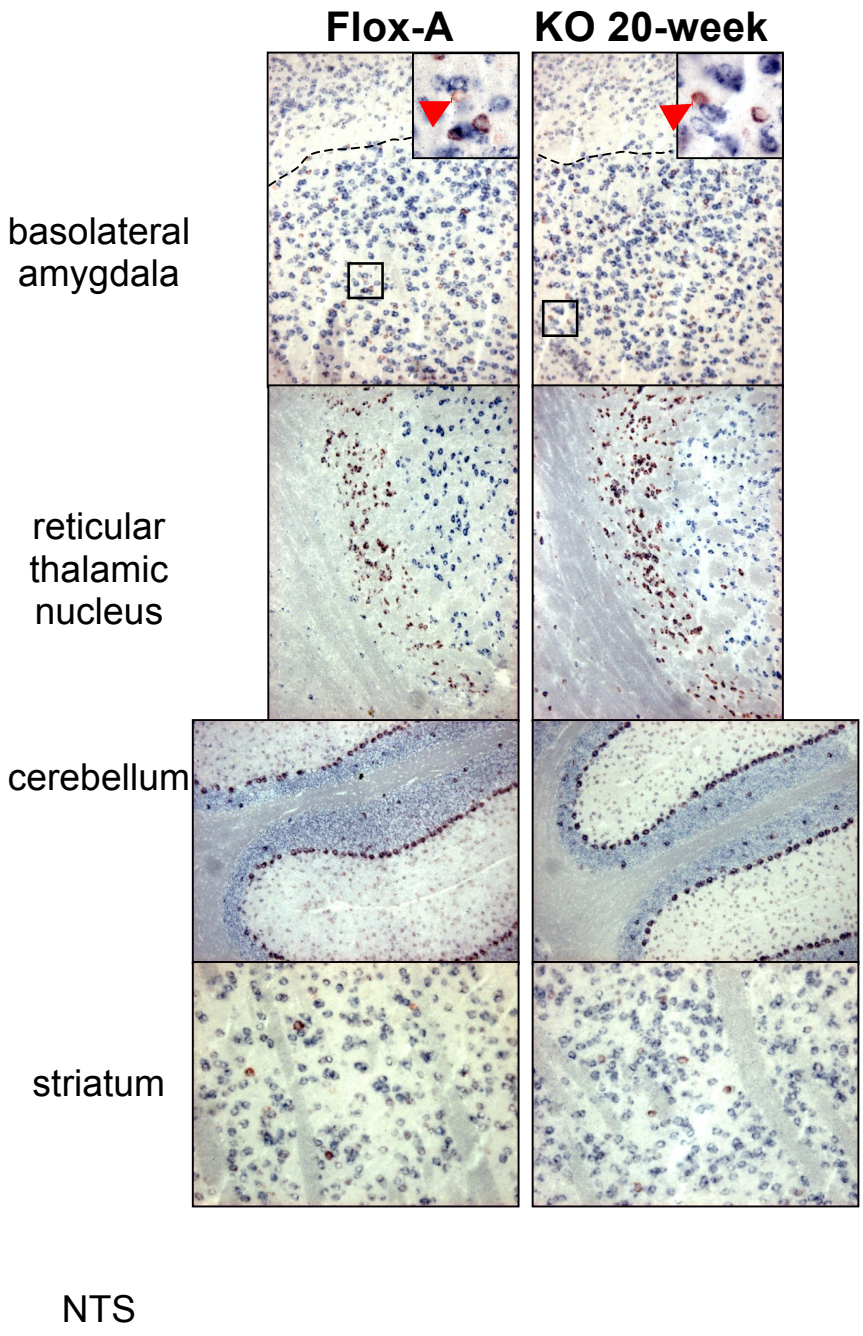

Supplementary Fig. 4 Photomicrographs from double *in situ* hybridization—Brain subregions. Hybridization of anti-*GAD67*-DNP probe and anti-*NR1*-DIG probe on parasagittal sections from 20-week-old mice. DIG signals were detected using NBT-BCIP (blue), and DNP signals were detected with peroxidase-AEC (red) after incubation with biotinylated anti-rabbit secondary antibody, followed by avidin-biotin complex formation. Brown color indicates colocalization of *GAD67* and *NR1* mRNAs. No significant difference in *NR1* mRNA-staining patterns of GABAergic neurons outside the corticolimbic areas was observed among genotypes. Inset in amygdala image depicts sporadic *GAD67* mRNA-positive cells without detectable levels of *NR1* mRNA in controls or mutants. NTS, nucleus tractus solitarius.

Nature Neuroscience: doi:10.1038/nn.2447

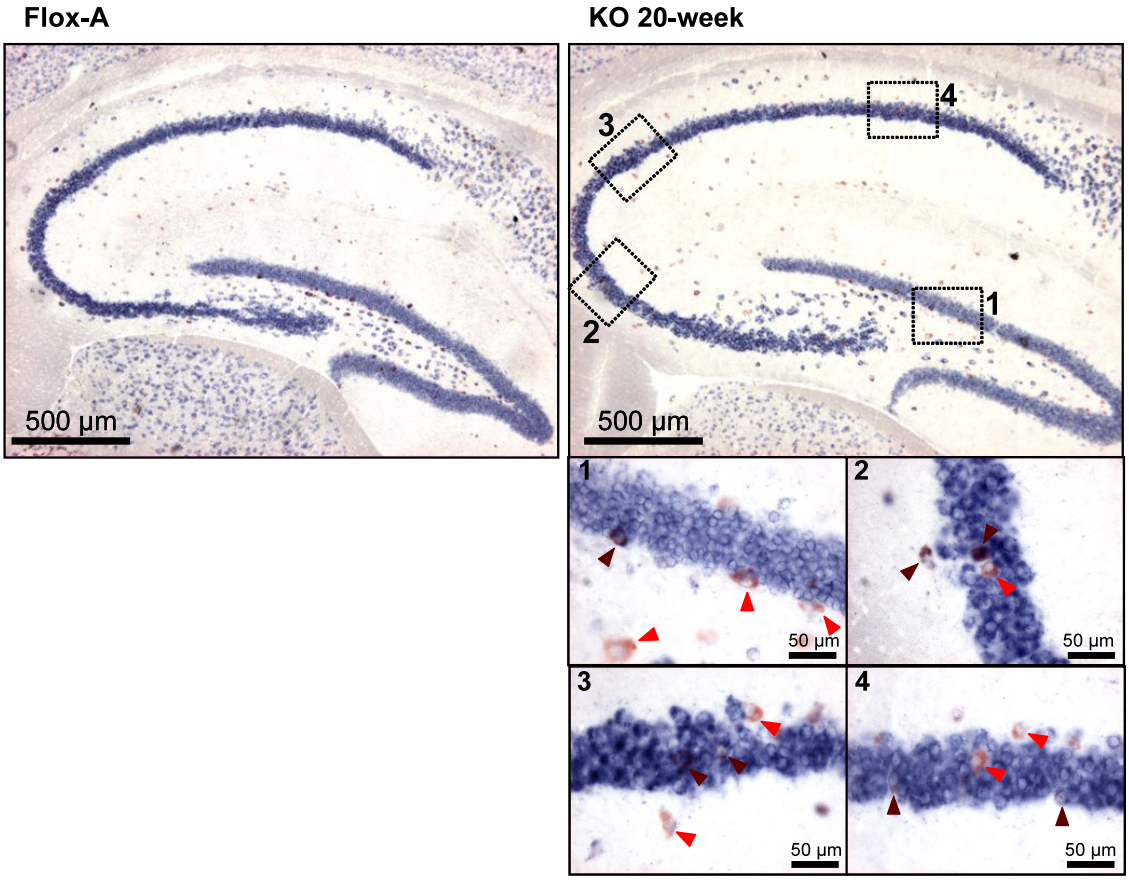

Supplementary Fig. 5 Photomicrographs from double *in situ* hybridization—Hippocampus. Upper row: low magnification showing no observable decrease in *NR1* mRNAs in hippocampal principal neurons from 20-week-old animals. Lower row: high magnification of boxed areas in mutants (1, dentate gyrus; 2, CA3; 3, CA2; 4, CA1). *GAD67* mRNA-positive neurons with no detectable *NR1* mRNA are indicated by red arrows. *GAD67* mRNA-positive neurons with *NR1* mRNA are indicated by brown arrows. DNP-labeled cRNA probe for *GAD67* (red); DIG-labeled cRNA probe for *NR1* (blue).

Nature Neuroscience: doi:10.1038/nn.2447

Supplementary Fig. 6 NMDA-mediated spontaneous EPSC in Cre-targeted GABAergic neurons.

(**a**) Immunohistochemical characterization of a neuron filled with biocytin (blue) during whole-cell voltage clamp recording in slice of primary somatosensory cortex (S1) from Cre-control mice (*Ppp1r2-cre*$^{+/-}$;*Rosa26-EYFP*$^{loxP/+}$). Cre-targeted neurons were visualized during the recording by EYFP expression produced by crossing with the *loxP*-flanked *Rosa26-EYFP* reporter[3], and later immunostained with anti-GFP (green) and/or anti-parvalbumin (PV: red). White arrow indicates triple colocalization (merge). (**b**) Electrophysiological characterization of the neuron in (**a**). Response of the membrane potential to injection of hyperpolarizing and depolarizing current steps. Steady interspike intervals observed during supra-threshold current steps in this example are typical of fast-spiking neurons. EYFP-positive neurons with low-threshold spiking patterns or regular spiking patterns were also detected (data not shown). (**c**) Whole-cell patch-clamp recordings[4] under different pharmacological conditions. Spontaneous EPSCs (sEPSCs) from the fast-spiking neuron in (**a-b**) are sensitive to D-APV, indicating functional NMDA currents in fast-spiking PV-positive interneurons in Cre-control mice. (**d**) Quantitative analysis of sEPSC amplitudes of Cre-targeted neurons from hippocampal area CA1 of Cre-control (*Ppp1r2-cre*$^{+/-}$; *Rosa26-EYFP*$^{loxP/+}$, n=9) and postnatal knockout mutant (*Ppp1r2-cre*$^{+/-}$; *NR1*$^{loxP/loxP}$-line A ; *Rosa26-EYFP*$^{loxP/+}$, n=9, KO) animals under baseline conditions, AMPA blockade (+NBQX), and AMPA/NMDA blockade (+NBQX/+APV). Mann-Whitney *U*-Test *p<0.01 vs Cre-control. (**e**) Quantitative analysis of the 63-30 % decay time of sEPSC under baseline conditions from cortex and hippocampus targeted neurons. The sEPSC from postnatal knockout mutants displayed a faster kinetic compatible with the absence of NMDAR-mediated currents. Mann-Whitney *U*-Test, *p<0.01 vs Cre-control. Data are presented as mean ± s.e.m.

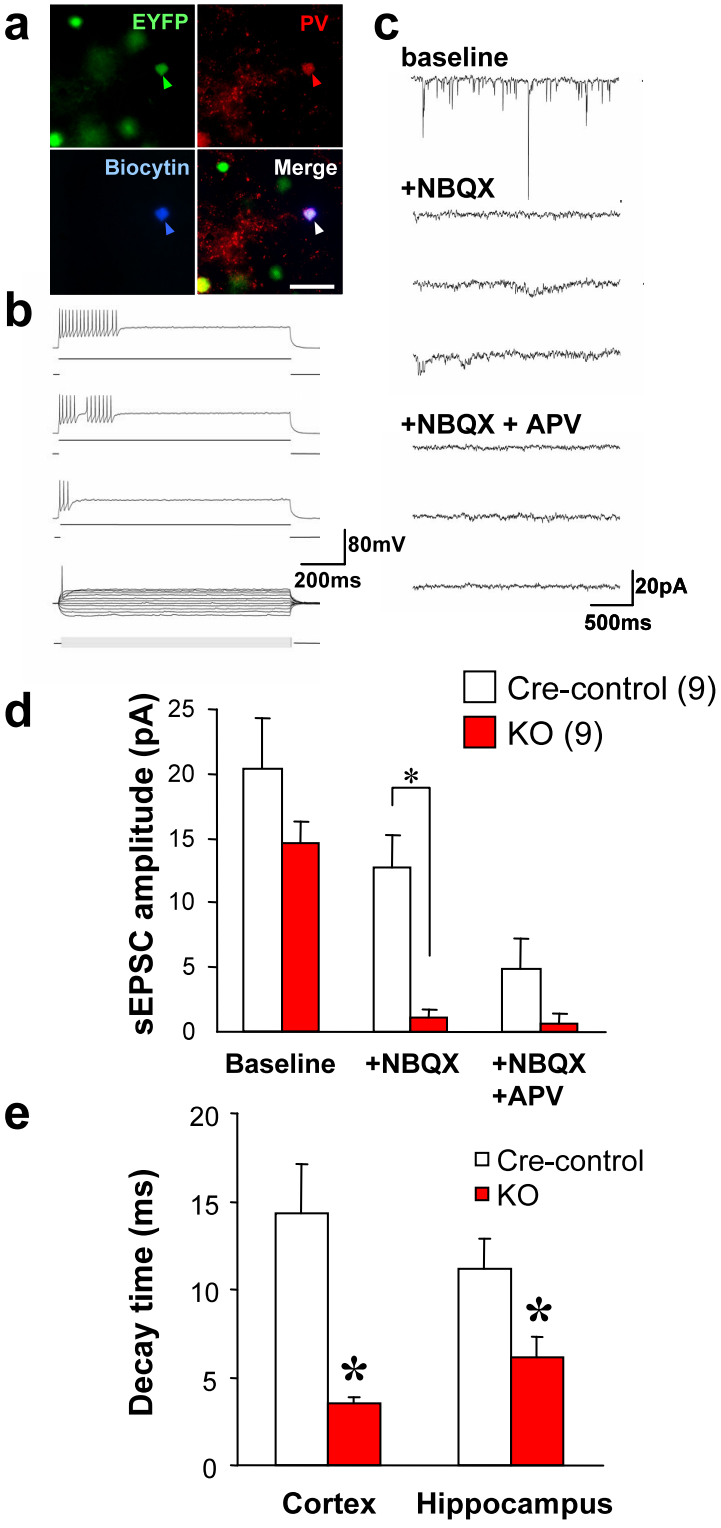

Nature Neuroscience: doi:10.1038/nn.2447

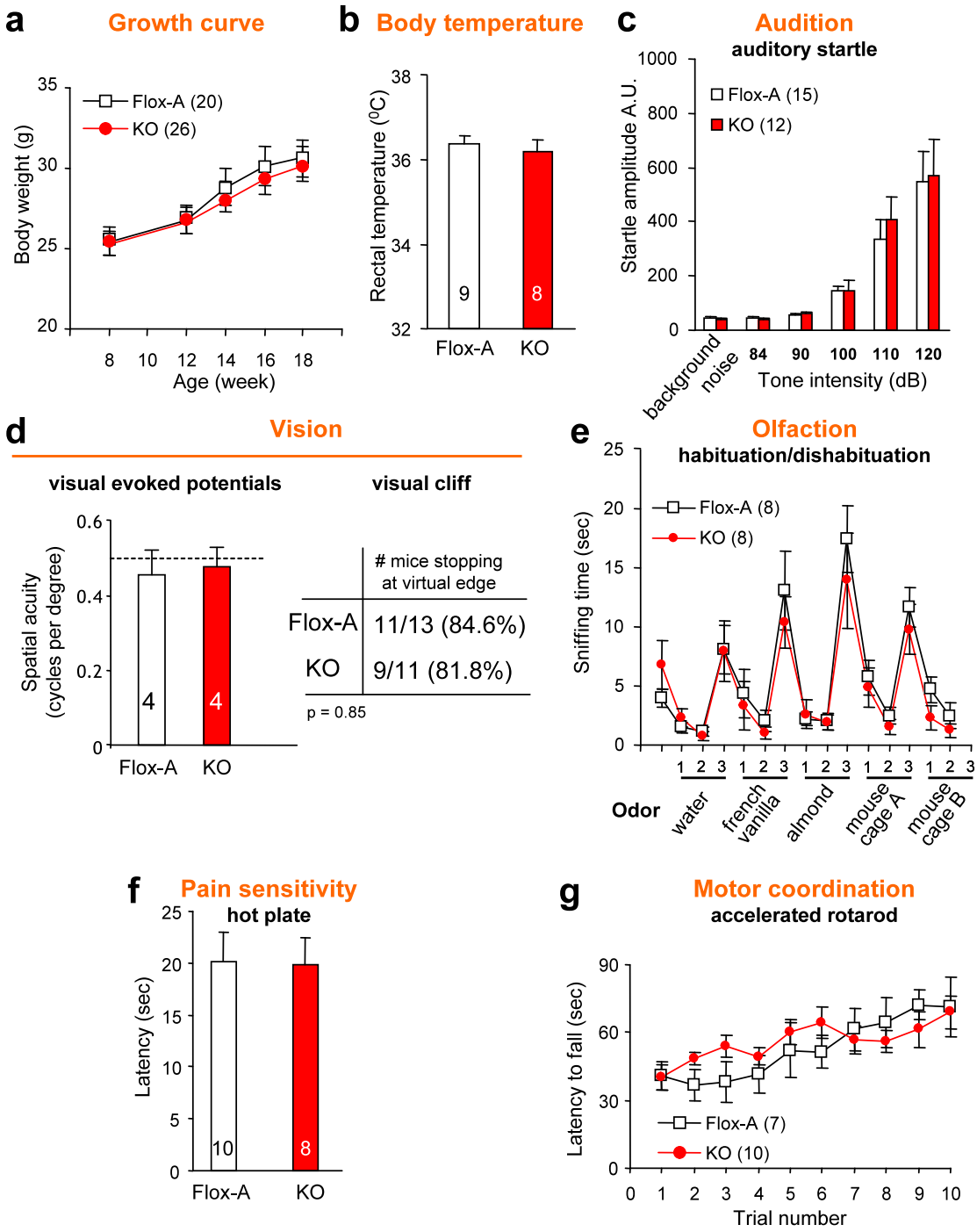

Supplementary Fig. 7 Assessment of basic physiological functions. (**a**)Assessment of general health, physical appearance, growth, neurological and sensory functions was performed in single-housed animals at 14 to 18 weeks of age as described[5]. All behavioral findings were confirmed in at least 2 separate cohorts of animals. No differences were observed in body weight between postnatal NR1 knockout mutants (*Ppp1r2-cre*$^{+/-}$; *NR1*$^{loxP/loxP}$-line A, KO) and Flox-A controls (*NR1*$^{loxP/loxP}$-line A) at any age. (**b**) Mutants' rectal temperature[6] did not differ from Flox-A controls, suggesting normal body temperature regulation in the mutants. (**c**) Auditory function was normal as assessed by auditory startle reflex[7]. We used a SR-LAB startle chamber (San Diego Instruments, San Diego, CA) consisting of a plexiglas cylinder mounted on a platform in a ventilated sound-attenuated cubicle. A high-frequency loudspeaker mounted on the ceiling produced all acoustic stimuli. Movements within the cylinder were detected and transduced by a piezoelectric accelerometer attached to the plexiglass base, and were digitized and stored automatically. Background sound levels (70 dB) and calibration of the acoustic stimuli were confirmed with a digital sound meter. The session began with a 5-min acclimation period follow by 42 trials, divided into 7 blocks of 6 trials each. Each block contained 1 no-stimulus trial and 5 trials with an auditory stimulus of different intensities (40 ms of white noise pulse at 84, 90, 100, 110, 120 dB) delivered in pseudo-random order with an average intertrial time of 15 s (10-20 s). Beginning at the stimulus onset, 65 readings of 1-ms duration were recorded to obtain the

Nature Neuroscience: doi:10.1038/nn.2447

peak startle amplitude. The average response was calculated for each trial. (**d**) Visual acuity assessed by visual evoked potential (VEP) recording under anesthesia[8], was normal in mutants. Briefly, the dura covering the binocular visual cortex (V1b; ~3.5 mm posterior to Bregma and 3.5 mm lateral to the midline) was exposed through a hole (~ 3mm diameter) in the skull following anesthesia via 2% to 3% isoflurane in 100% O_2 delivered via a small nose tube. Electrode placement on the binocular region of V1 was confirmed by capturing a VEP in response to stimulation of the ipsilateral eye. The visual stimuli were full-screen vertical-square wave gratings of a range of spatial frequencies reversing at 1 Hz, with 96.28% maximal contrast, presented on a computer monitor 25 cm from eyes, in a darkened room. The amplitude of the primary positive component of the VEP (~150 ms latency) was amplified (1000x), filtered (300 Hz low pass digital filter), and averaged in synchrony with the stimulus using OpenEx software (100 – 300 trials). To estimate spatial acuity, the VEP amplitude was plotted against the spatial frequency of the visual stimulus, and the linear regression was extrapolated to zero VEP amplitude. Visual perception was evaluated in the visual cliff test conducted in a box with a ledge[9]. The inner surface of the box and ledge were covered with black and white checkerboard (2.5 x 2.5 cm) contact paper, to emphasize the ledge drop-off (60 cm high). A piece of clear plexiglass spans the ledge, resulting in the visual appearance of a cliff. Blind animals walk across the plexiglas without stopping. Each trial was initiated by placing the mouse, with trimmed whiskers, on the middle of the "safe" side. The behavior was scored as "positive" when the mouse stopped at the virtual edge before attempting to cross. Percentage of animals stopping at the edge was quantified. Each animal was tested only once. (**e**) Ability to recognize social and non-social odors, as assessed by the olfactory habituation/dishabituation task[10,11] was normal in controls and mutants. Swabs were dipped in (1) tap water, (2) French vanilla extract (McCormick, Hunt Valley, MD; 1:200 dilution), (3) almond extract (1:200), (4) the bottom surface of a plastic cage that contained an unfamiliar group of C57BL/6N male mice for 6 d, and (5) a second unfamiliar mouse cage. (**f**) No differences were observed in pain sensitivity as assessed by the hot plate test[12] using a Hot Plate Analgesia Meter (Columbus Instruments). Mice were placed on the hot plate (55±0.1 ^{o}C). The mice were constrained to the hot plate by clear acrylic walls (19 cm tall, open top). The latency to respond with either hindpaw lick, hindpaw flick, or jump was measured and the mouse was immediately removed from the hot plate and returned to its home cage. The cut-off time was 30 s. Animals were tested individually and were not habituated to the apparatus prior to testing. (**g**) Balance and motor coordination were normal for mutants and controls, as assessed by the accelerating rotarod test[13] using an Accurotor rotarod (AccuScan Instruments). Animals were tested concurrently in 4 separate 11 cm-wide compartments on a rod approximately 3 cm in diameter and elevated 35 cm. The apparatus started at an initial speed of 4 rpm and gradually accelerated at a rate of 0.2 rpm/s. The latency to fall from the rod was recorded with a cut-off time of 2 min. Each animal was assessed over ten trials with 20-min intertrial intervals. Data are presented as mean ± s.e.m.; number of animals is indicated between parentheses or inside plot bars.

Nature Neuroscience: doi:10.1038/nn.2447

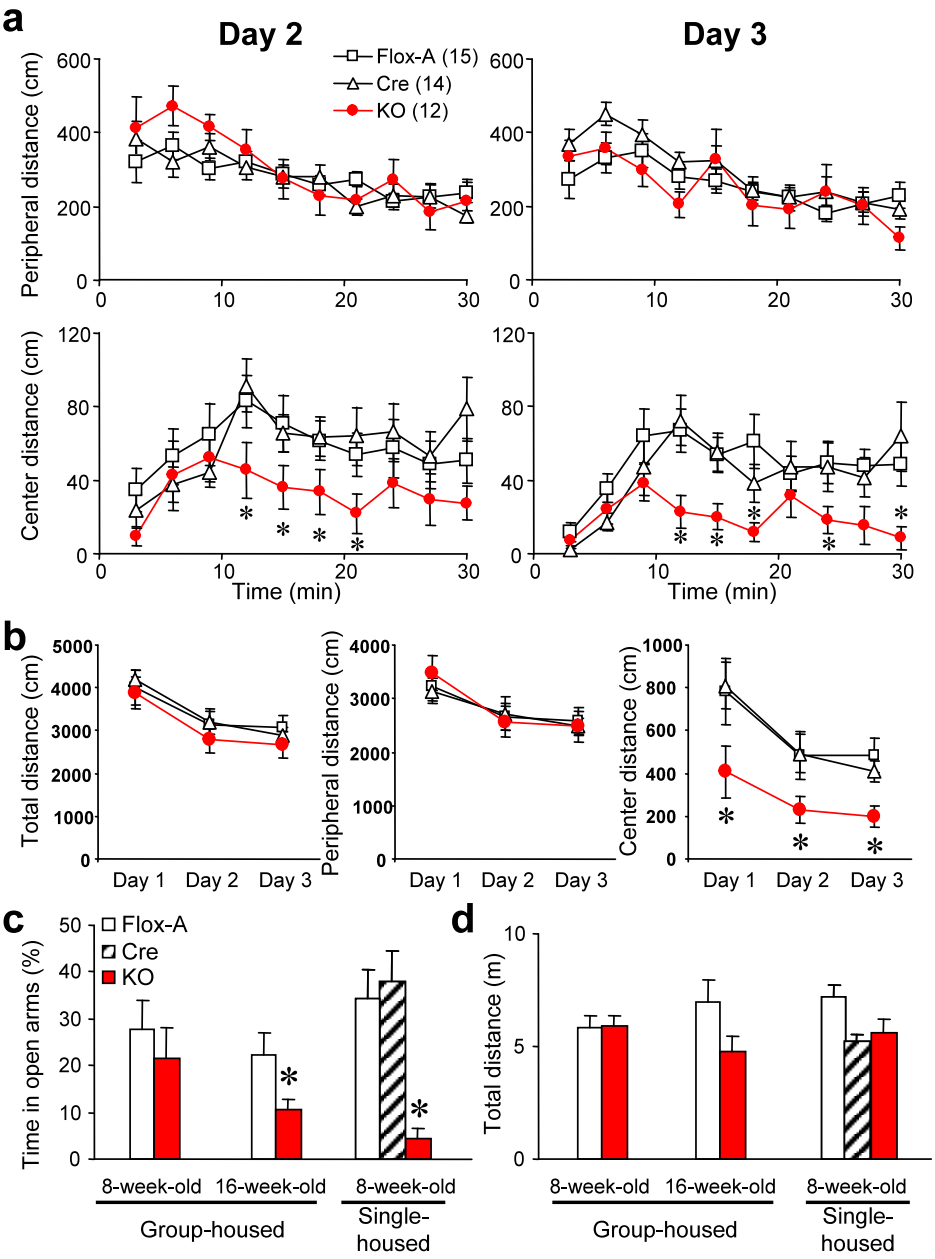

Supplementary Fig. 8 Supplementary data for open field activity and elevated plus maze task. (**a**) Novelty induced-hyperlocomotion observed over 5 min of exploration in a new open field in postnatal NR1 knockout mutants (*Ppp1r2-cre*$^{+/-}$; *NR1*$^{loxP/loxP}$-line A, KO) disappeared with re-exposure to the same arena (Day 2 and Day 3) while exploration of the center area of the arena remained significantly reduced. (**b**) Total, peripheral, and center distance accumulated in each session across 3 consecutive days of testing in an open field. No differences were observed across genotypes for accumulated total or peripheral distance, reflecting normal locomotor function. Center distance was significantly decreased across days, suggesting that the anxiety-like phenotype was independent of the novelty of the environment. *p<0.05 vs Flox-A and Cre, Repeated measures ANOVA/LSD post-hoc test, genotype factor $F_{2,76}$=4.4 P<0.05. (**c**) In the elevated plus maze test, group-housed mutants at 16 weeks of age (but not at 8-week-old) spent less time in open arms, suggesting anxiety-like behavior. *p<0.05 vs Flox-A, LSD test after two-way ANOVA with significant interaction $F_{1,42}$ =4.21 p<0.05. Single-housed mutants presented an anxiety-like phenotype at 8 weeks of age, suggesting social isolation stress-induced anxiety. *p<0.001 vs Cre and Flox-A, LSD test after one-way ANOVA $F_{2,35}$=10.8 p<0.0005. (**d**) Postnatal knockout mutants displayed normal locomotor activity in the elevated plus maze test regardless of age and housing conditions.

Nature Neuroscience: doi:10.1038/nn.2447

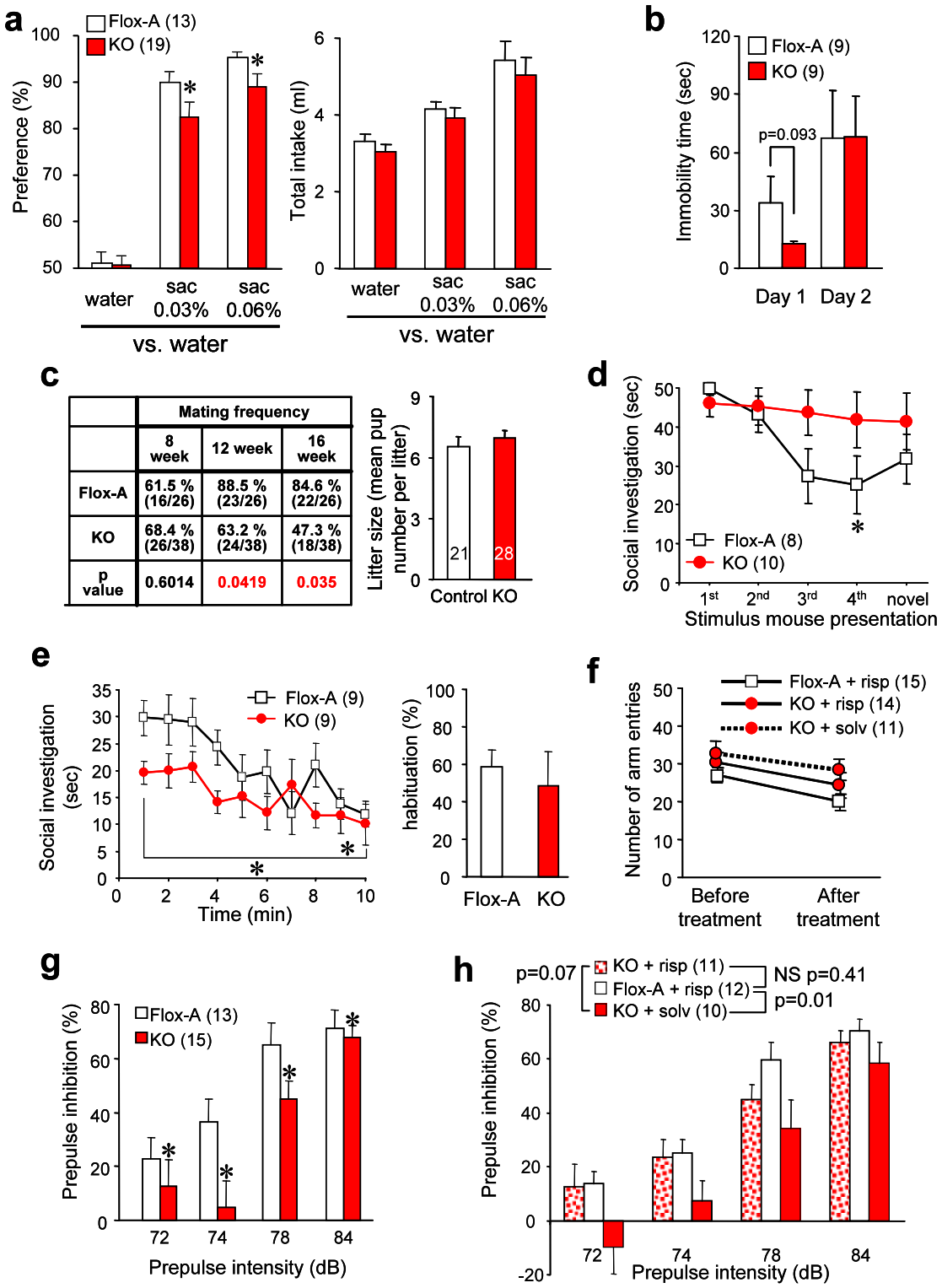

Supplementary Fig. 9 Supplemental data for other behavioral testing using postnatal knockout mutants. (**a**) Social isolation induced an anhedonia-like phenotype. Postnatal NR1 knockout mutants (*Ppp1r2-cre*$^{+/-}$; *NR1*$^{loxP/loxP}$-line A) at 16-week-old displayed a decreased preference for saccharine solutions in a two-bottle preference test after 8 weeks of single-housing. Total liquid intake was normal, suggesting that anhedonia-like phenotype in the mutants was not due to abnormal liquid consumption. Repeated measures ANOVA/LSD *post hoc* test, *p<0.05 vs Flox-A. During 6 days of the experiment, mice were kept single-housed in their home cage and had access to two drinking spouts connected to 30-ml graded pipettes[14]; one containing deionized water and another containing water/saccharine solution [either 0.033%, or 0.066% w/v (tube design and construction, see http://www.monell.org/MMTPP/)]. The test schedule was as follows: Day 1-2, water vs. water; Day 3-4, water vs. saccharine 0.033%; and Day 5-6, water vs. saccharine 0.066%. The position of the tubes was switched every 24 hr to prevent any possible side bias. Raw values were corrected for volume loss by evaporation and leakage (0.25

Nature Neuroscience: doi:10.1038/nn.2447

ml/72 hr on average) assessed in an empty cage. For each mouse on each day, solution preference ratios were calculated based on the formula: Preference (%) = saccharine intake/(saccharine intake+ water intake) x 100. The sum of saccharine intake and water intake was also evaluated as total intake. Animals were single-housed at 8 weeks of age and tested after 1, 4, and 8 weeks after single housing. Animals were single-housed in home cages during the periods between testing. (**b**) Two-day forced swim test[15,16] revealed a tendency towards decreased immobility only during the first day of testing, perhaps reflecting stress-induced psychomotor agitation. Twelve-15-week-old male mice were assessed for depression-related behavior using a modified version of the mouse forced swim test, in which subjects were repeatedly exposed to the swim stressor. On Day 1, mice received a single 15-min forced swim stress exposure to a transparent plexiglas cylinder (30 cm high, 20 cm in diameter) filled with 23-25°C water. On Day 2, mice received a second session of 6-min. Sessions were video recorded and passive immobility (cessation of movement except minor involuntary movements of the hindlimbs) was measured during minutes 2 to 6 on each day by an observer blind to genotype. Repeated measure ANOVA, $F_{1,16}$=0.97 for interaction, p=0.33. (**c**) Impaired mating performance in single-housed mutants. Copulatory behavior was assessed as described[17]. In brief, single-housed males were mated with a 4-week-old C57BL/6N naïve female (Taconic Farms) that had been treated with pregnant mare serum (PMS) and human chorionic gonadotropin (hCG) to induce ovulation. The female mice were examined for the presence of copulation plugs the following morning. Each male was tested twice within a week and mating efficiency was calculated as percentage of plugged females over total number of female presentations per genotype. *P* value by X^2 test. Mean number of pups per litter was normal when compared with control animals, suggesting normal reproduction. (**d**) Social recognition test conducted in the home cage of the test mice. Flox-A mice showed a decrease in the amount of time dedicated to social investigation[18] of the stimulus mouse along successive exposures (1 min presentation, 10 min intertrial interval). In contrast, mutants displayed no significant habituation across trials, consistent with the data in **Fig. 3e**. Note that mutants displayed a normal level of social investigation during the first presentation, in contrast to the results obtained in a neutral cage (**Fig. 3e**). Repeated measures ANOVA/LSD *post hoc* test, *p<0.05 vs. Flox-A. (**e**) Continuous social recognition in a neutral cage. To focus on the short-term memory component of this task, a different cohort of mice (12-14 week-old) was habituated to a clean cage for 1 hr and a stimulus male was placed in the cage for 10 min. The session was video recorded and every minute of social investigation was quantified off-line, as habituation index = social investigation time during the last min/ social investigation time during the first min x100. Social investigation of a stimulus mouse by mutants declined during the 10-min continuous exposure despite of an initial low investigation levels for first 3-min. Right panel; No significant differences in habituation of social investigation were detected between groups. (**f**) Chronic treatment with risperidone, which was sufficient to restore normal working memory in mutants during a Y maze spontaneous alternation task (**Fig. 3h**), produced no significant alterations in locomotor activity. The slight decrease observed in all groups (including solvent-treated) before and after treatment was probably due to suppression of locomotor activity by risperidone[19]. Repeated measures ANOVA, $F_{2,37}$=0.13 for interaction, *P*=0.87. Risperidone treatment: 2.5 mg/kg/day in drinking water continuously for 3 weeks freshly made every 72 hr, control mice received solvent (0.1% acetic acid neutralized to pH 7.4-7.6). Risperidone dose was chosen because plasma levels were equivalent to those observed in the human therapeutic range[20]. (**g**) Group-housed mutants presented a deficit in the prepulse inhibition (PPI) of the auditory startle reflex across the prepulse intensities, suggesting that PPI impairment in the mutants was not stress-dependent. Two-way ANOVA, $F_{1,104}$=8.3 for genotype factor, p<0.005. (**h**) Chronic treatment with risperidone partially rescued the PPI deficit observed in the mutants. Repeated measures ANOVA, $F_{2,90}$=3.71 p=0.03 for treatment factor (LSD *post hoc* comparisons are indicated in graph legend); $F_{6,90}$=0.69, p=0.65 for interaction. Data are presented as mean ± s.e.m.; number of animals is indicated in parentheses or inside plot bars.

Nature Neuroscience: doi:10.1038/nn.2447

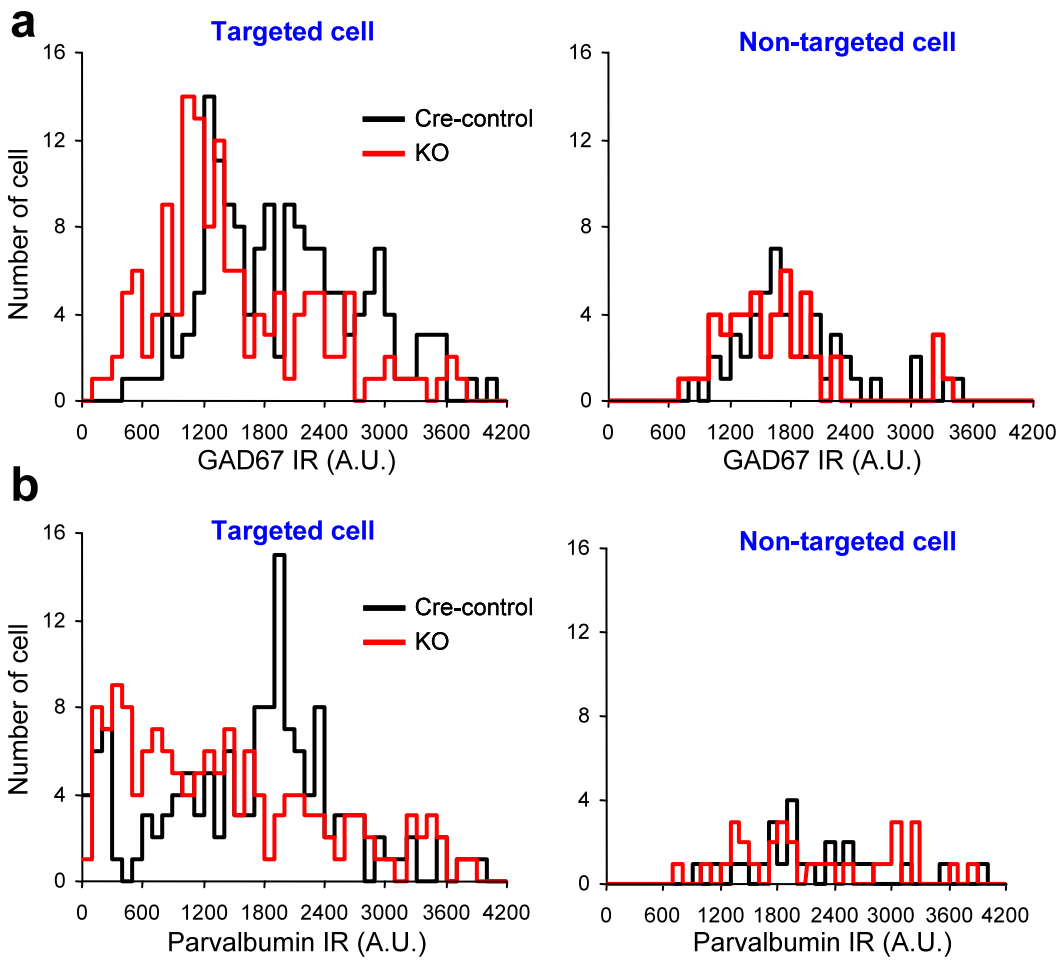

Supplementary Fig. 10 Evaluation of GAD67 and parvalbumin immunoreactivity. (**a** and **b**) Histograms showing GAD67 immunoreactivity (IR) (**a**) and parvalbumin IR (**b**) distribution in Cre-targeted (EYFP-positive) and Cre non-targeted (EYFP-negative) neurons of Cre-control (*Ppp1r2-cre*$^{+/-}$; *Rosa26-EYFP*$^{loxP/+}$) and postnatal NR1 knockout mutant (*Ppp1r2-cre*$^{+/-}$; *NR1*$^{loxP/loxP}$-line A; *Rosa26-EYFP*$^{loxP/+}$) mice. Note the shift toward lower values for Cre-targeted neurons in the mutants compared to the control values. The mutant non-targeted population overlapped with that of the control population. A distinct subpopulation of targeted neurons in Cre-control animals had significantly low levels (IR < 400 AU) of parvalbumin IR; 400 A.U. was used to define the threshold for neuron inclusion (IR > 400 AU) in the parvalbumin IR analysis. Notably, Cre-targeted neurons represented 83.5% of parvalbumin-positive interneurons in S1 layer II/III of the Cre-controls (n=5) that were crossed with the *loxP*-flanked *Rosa26-EYFP* mice, suggesting higher frequency of Cre recombination in the parvalbumin-positive neurons in the *loxP*-flanked *Rosa26-EYFP* mice than in the *loxP*-flanked *Rosa26LacZ* mice (**Fig. 1h**). A.U., Arbitrary Unit.

Nature Neuroscience: doi:10.1038/nn.2447

Supplementary References:

1. Soriano, P. Generalized lacZ expression with the ROSA26 Cre reporter strain. *Nat. Genet.* **21**, 70-71 (1999).
2. Benson, D.L., Isackson, P.J., Gall, C.M. & Jones, E.G. Contrasting patterns in the localization of glutamic acid decarboxylase and Ca2+/calmodulin protein kinase gene expression in the rat central nervous system. *Neuroscience* **46**, 825-849 (1992).
3. Costantini, F. Cre reporter strains produced by targeted insertion of EYFP and ECFP into the ROSA26 locus. *BMC. Dev. Biol.* **1**, 4, (2001).
4. Zsiros, V., Aradi, I. & Maccaferri, G. Propagation of postsynaptic currents and potentials via gap junctions in GABAergic networks of the rat hippocampus. *J. Physiol* **578**, 527-544 (2007).
5. Crawley, J.N. Behavioral phenotyping of transgenic and knockout mice: experimental design and evaluation of general health, sensory functions, motor abilities, and specific behavioral tests. *Brain Res.* **835**, 18-26 (1999).
6. Boulay, D., Depoortere, R., Rostene, W., Perrault, G. & Sanger D.J Dopamine D3 receptor agonists produce similar decreases in body temperature and locomotor activity in D3 knock-out and wild-type mice. *Neuropharmacology* **38**, 555-565 (1999).
7. Duncan, G.E. *et al.* Deficits in sensorimotor gating and tests of social behavior in a genetic model of reduced NMDA receptor function. *Behav. Brain Res.* **153**, 507-519 (2004).
8. He, H.Y., Ray, B., Dennis, K. & Quinlan, E.M. Experience-dependent recovery of vision following chronic deprivation amblyopia. *Nat. Neurosci.* **10**, 1134-1136 (2007).
9. Salinger, W.L., Ladrow, P. & Wheeler, C. Behavioral phenotype of the reeler mutant mouse: effects of RELN gene dosage and social isolation. *Behav. Neurosci.* **117**, 1257-1275 (2003).
10. Luo, A.H. *et al.* Impaired olfactory behavior in mice deficient in the alpha subunit of G(o). *Brain Res.* **941**, 62-71 (2002).
11. Wrenn, C.C., Harris,A.P., Saavedra,M.C. & Crawley,J.N. Social transmission of food preference in mice: methodology and application to galanin-overexpressing transgenic mice. *Behav. Neurosci.* **117**, 21-31 (2003).
12. Mogil, J.S. *et al.* Heritability of nociception I: responses of 11 inbred mouse strains on 12 measures of nociception. *Pain* **80**, 67-82 (1999).
13. Dang, M.T. *et al.* Generation and characterization of Dyt1 DeltaGAG knock-in mouse as a model for early-onset dystonia. *Exp. Neurol.* **196**, 452-463 (2005).
14. Bachmanov, A. A., Tordoff, M. G. & Beauchamp, G. K. Sweetener preference of C57BL/6ByJ and 129P3/J mice. *Chem. Senses* **26**, 905-913 (2001).
15. Porsolt, R.D., Bertin, A. & Jalfre, M. Behavioral despair in mice: a primary screening test for antidepressants. *Arch. Int. Pharmacodyn. Ther.* **229**, 327-336 (1977).
16. Wellman, C.L. *et al.* Impaired stress-coping and fear extinction and abnormal corticolimbic morphology in serotonin transporter knock-out mice. *J. Neurosci.* **27**, 684-691 (2007).
17. Mohn, A.R., Gainetdinov, R.R., Caron, M.G. & Koller, B.H. Mice with reduced NMDA receptor expression display behaviors related to schizophrenia. *Cell* **98**, 427-436 (1999).
18. Ferguson, J. N. *et al.* Social amnesia in mice lacking the oxytocin gene. *Nat. Genet.* **25**, 284-288 (2000).
19. Bardgett, M.E., Baum, K.T., O'Connell, S.M., Lee, N.M. & Hon, J.C. Effects of risperidone on locomotor activity and spatial memory in rats with hippocampal damage. *Neuropharmacology* **51**, 1156-1162 (2006).
20. Terry, A.V., Jr. *et al.* Oral haloperidol or risperidone treatment in rats: temporal effects on nerve growth factor receptors, cholinergic neurons, and memory performance. *Neuroscience* **146**, 1316-1332 (2007).

Nature Neuroscience: doi:10.1038/nn.2447